Bacterially mediated removal of phosphorus and cycling of nitrate and sulfate in the waste stream of a "zero-discharge" recirculating mariculture system

M.D. Krom[a,b], , A. Ben David[c], E.D. Ingall[d], L. G. Benning[a], S. Clerici[a] , S. Bottrell[a], C. Davies[a] , N. J. Potts[a], R.J.G. Mortimer[a] , J. van Rijn[c*]

[a]School of Earth and Environment, Leeds University, UK ; [b]Charney School of Marine Sciences, Haifa University, Israel; [c]The Robert H. Smith Faculty of Agriculture, Food and Environment, The Hebrew University of Jerusalem, Rehovot, Israel; [d]School of Earth and Atmospheric Sciences, Georgia Institute of Technology, Atlanta, USA

*Corresponding author. The Robert H. Smith Faculty of Agriculture, Food and Environment, P.O.Box 12, Rehovot 76100, Israel; email: jaap.vanrijn@mail.huji.ac.il; tel.: +972-8-9489302; fax: +972-8-9489024

22 **Abstract**

23 Simultaneous removal of nitrogen and phosphorus by microbial biofilters has been

24 used in a variety of water treatment systems including treatment systems in

25 aquaculture. In this study, phosphorus, nitrate and sulfate cycling in the anaerobic

26 loop of a zero-discharge, recirculating mariculture system was investigated using

27 detailed geochemical measurements in the sludge layer of the digestion basin. High

28 concentrations of nitrate and sulfate, circulating in the overlying water (~15 mM),

29 were removed by microbial respiration in the sludge resulting in a sulfide

30 accumulation of up to 3 mM. Modelling of the observed S and O isotopic ratios in the

31 surface sludge suggested that, with time, major respiration processes shifted from

32 heterotrophic nitrate and sulfate reduction to autotrophic nitrate reduction. The much

33 higher inorganic P content of the sludge relative to the fish feces is attributed to

34 conversion of organic P to authigenic apatite. This conclusion is supported by: (a) X-

35 ray diffraction analyses, which pointed to an accumulation of a calcium phosphate

36 mineral phase that was different from P phases found in the feces, (b) the calculation

37 that the pore waters of the sludge were highly oversaturated with respect to

38 hydroxyapatite (saturation index = 4.87) and (c) there was a decrease in phosphate

39 (and in the Ca/Na molar ratio) in the pore waters simultaneous with an increase in

40 ammonia showing there had to be an additional P removal process at the same time

41 as the heterotrophic breakdown of organic matter.

42

43 Keywords: aquaculture; anaerobic sludge; phosphorus removal; denitrification; apatite

44 formation; sulfur cycling.

2

1. Introduction

Fish cages, a widely used industrial mariculture technology, typically discharge up to 80% of the nitrogen and phosphorus that is supplied in the feed into the environment (Naylor et al., 1998; van Rijn, 2013). Land based mariculture offers more control of the waste, but is often limited by the shortage of coastal sites and the cost of inland pumping of seawater and its discharge. The "Zero-Discharge System" (ZDS) is a recently developed sustainable mariculture system (Gelfand et al., 2003) which uses natural microbial processes to control water quality (Cytryn et al., 2003; Gelfand et al., 2003; Neori et al., 2007). The system operates in a completely sealed way, meaning that only a small amount of freshwater is used to replace losses by evaporation. There is no continuous or even intermittent discharge of aqueous effluent to the environment as exists in other mariculture systems. Although the advantages of ZDS mariculture systems in terms of waste output are clear, the mechanisms behind the nitrogen, sulfur and phosphorus cycling in such systems are not well understood.

The ZDS consists of two water treatment loops (Fig. 1). The aerobic loop converts toxic ammonia produced by fish to nitrate by means of a trickling biofilter. In the second loop, an anaerobic loop, consisting of a digestion basin (DB) and fluidized bed reactor, particulate waste organic matter (principally fish feces) and other nutrients are metabolized to environmentally harmless forms. Previous studies on this and similar systems revealed that the major processes affecting the overall water quality are nitrification in the aerobic treatment loop and bacterial breakdown of organic matter by processes including heterotrophic nitrate and sulfate reduction as well as autotrophic nitrate reduction coupled to sulfide oxidation in the DB and

3

70 fluidized bed reactor (Gelfand et al., 2003; Cytryn et al., 2005; Neori et al., 2007;

71 Sher et al., 2008; Schneider et al., 2011). However the relative contribution of these

72 anaerobic bacterial processes was not known. Around 70% of the C and N supplied

73 is lost as carbon dioxide and gaseous nitrogen species, presumed to be the result of

74 heterotrophic bacterial respiration (Neori et al., 2007). Of the phosphorus supplied

75 with the fish feed, 21% is taken up for fish growth. Only 5% of the remaining

76 phosphorus accumulates in the water column while the rest is present as solid and

77 pore water phosphorus, mainly in the DB sludge accumulating in the anaerobic

78 treatment loop. It was not known in what form this P accumulates in the sludge nor

79 what processes are controlling this accumulation.

80   Simultaneous removal of nitrogen (N) and phosphorus (P) by microbial

81 biofilters has been used in a variety of water treatment systems to treat nutrient-rich

82 waste streams. These include systems that use alternating aerobic-anaerobic

83 conditions to trap phosphate as polyphosphate under aerobic (van Loosdrecht et al.,

84 1997) or denitrifying conditions (van Loosdrecht et al., 1998) and release it in a

85 controlled way during the anaerobic cycle. The DB of the ZDS system has free

86 oxygen in the overlying water while the sludge itself is anaerobic with the precise

87 location of the redox boundary depending on the balance of recycling processes

88 within the system. In the DB examined in this study, N and P were found to be

89 simultaneously removed from the waste stream by the accumulation of P in

90 denitrifying organisms under entirely anoxic conditions (Barak and van Rijn, 2000a,

91 2000b; Barak et al., 2003; Neori et al., 2007).

92   Similar microbial processes to those in the digestion basin, may occur in

93 natural marine systems particularly in sediments underneath the upwelling regions of

94 the world such as the Benguela current off Namibia and off Oman in the Arabian

4

95   Sea. These locations have high concentrations of organic matter in the sediment (up

96   to 40%), much of which is labile causing high rates of heterotrophic bacterial activity

97   including sulfate reduction and methane production (Schulz et al., 1999).

98   Phosphorite (diagenetic apatite) nodules often form in the sediments beneath these

99   upwelling regions. Two processes have been suggested for this apatite formation.

100   Schenau et al. (2000) suggested that diagenic apatite was formed in pore waters

101   where phosphate released by heterotrophic respiration of organic matter created

102   high enough phosphate concentrations to overcome the kinetic barrier to apatite

103   formation (Van Cappellen and Berner, 1991). More recently, an alternative process

104   has been suggested in which bacteria, particularly sulfide oxidizing bacteria,

105   accumulate polyphosphate, which is then rapidly converted into diagenetic apatite

106   (Goldhammer et al., 2010). Both processes represent a shunt of P from its dissolved

107   form into bacterial biofilms, which is subsequently converted into mineral apatite.

108   This study examines the types and location of processes that control nitrate,

109   sulfate and phosphorus cycling within the sludge of the anaerobic loop in the ZDS

110   system. The major microbial transformations in the DB were determined using

111   detailed geochemical measurements of the depth distribution of relevant

112   geochemical parameters and their stable isotope composition in the DB sludge layer

113   and the overlying water. Detailed measurements of P in the sludge, pore and

114   overlying waters were made using geochemical and mineralogical methods to

115   determine the P speciation and its changes with depth. The identified P cycling

116   processes are compared and contrasted with similar processes in natural and

117   engineered systems.

118

119

2. Material and Methods

121

2.1. System description

123

The zero discharge system (ZDS) in this study was an enlarged version of the system previously described in detail by Gelfand et al. (2003). Briefly, the system comprised a fish basin (5 m^3) stocked with the gilthead seabream (*Sparus aurata*) from which water was circulated through aerobic and anaerobic treatment compartments (Fig. 1). The aerobic compartment consisted of a trickling filter with a volume of 8 m^3 and a surface area of 1,920 m^2. Water from the trickling filter was collected in a trickling filter basin (3m^3) which was situated directly underneath the trickling filter. Surface water from the fish basin was circulated through the aerobic compartment at a rate of 10 m^{3}h^{-1}. The digestion basin (DB, gross volume: 5.4 m^3) was the main part of the anaerobic treatment compartment. Water from the bottom of the fish basin was drained continuously (0.8 m^{3}h^{-1}) into the DB. Effluent water from the DB was recirculated (0.8 m^{3}h^{-1}) through a fluidized bed reactor (FBR, volume: 13 L) before being returned to the Intermediate Collection Basin. The FBR removes any sulfide or other reduced potentially toxic compounds by microbial oxidation before they reach the fish tank. The DB, with a total surface area of 3.64 m^2 (2.6 m length; 1.4 m width), contained a partition in the middle of the basin causing the incoming water to flow over a total length of 5.2 m before leaving the basin. Total depth of water and sludge in the DB was 80 cm and sludge thickness ranged between 30 and 50 cm (i.e. the water layer overlying the sludge varied in thickness from 30 to 50 cm). As no continuous water exchange is required, the system can be operated away

from a seawater source. In the absence of such a source and to meet the desired water salinity, solid sea salt (Red Sea pHarm Ltd, Israel) was initially added to the DB to reach a final concentration of ~8,500 mgNa/L (i.e. 20 ± 2 ppt) in the system water. It was allowed to dissolve there and diffuse into the overlying water. Local Rehovot tap water was periodically added to the system to compensate for evaporative losses. The system was started in October 2011 with sludge already present from previous operations of the ZDS over the past seven years. This was done to avoid an unacceptably long induction period since we added small fish at first and thus there was limited waste organic matter being supplied to the DB. On October 31, 2010, 738 fish were stocked with an initial weight of 1.5 g and on October 16, 2011, 668 fish were harvested with an average weight of 237.6 g. Feed addition over this period was 241 kg. Hence, the feed conversion coefficient (i.e. total feed addition divided by to the total fish weight gained) was 1.53

2.2. In situ *sampling*

Water quality parameters sampled in the fish basin were recorded for a period of 360 days starting in October 2011. Oxygen and temperature were measured daily while ammonia, nitrite, nitrate, phosphate, pH and alkalinity were analyzed weekly. The sediment system was sampled when anaerobic conditions had been clearly established in the DB sludge (based on removal of nitrate from the overlying water; see Fig S1).

Core samples of sludge from the DB were taken four times from the same location in the digestion basin (see Fig. 1) using a custom-built corer with a rubber diaphragm to seal the bottom. These cores were used for subsequent solid and

7

169   macropore water analysis. Cores were taken during the morning of July 12th (pore

170   water chemistry and solid analyses), July 13th (for pH) and two cores for isotopic

171   analyses were taken on August 4th (Core A) and February 2nd, 2012 (core B). The

172   first collected core (July 12th, 2011) was taken back to the laboratory and frozen at -

173   20°C. After 24 hours the frozen core was partially thawed (~20 minutes) and sections

174   of 1 cm each were extruded from the bottom of the core and sliced off with a metal

175   saw. The largest part of the sludge disk was placed in a pre-weighed 50 ml

176   centrifuge tube. It was weighed (wet weight) and then centrifuged for 15 minutes at

177   3,500 rpm at 4°C. The supernatant pore waters were filtered through a 0.45 μm filter

178   for phosphate, ammonia and nitrate determination. A subsample was refrozen for

179   subsequent analysis. After thawing, a small known amount of acid was added to the

180   tubes. The acidified samples well mixed, weighed accurately so that the volume of

181   dilution by acid could be determined, and analysed by Inductively Coupled Plasma

182   Atomic Emission Spectroscopy (ICP-AES) for Na, Ca, Mg, P and S. A wet sludge

183   subsample was weighed for porosity determination and then frozen for subsequent

184   freeze-drying. The freeze-dried samples were used for all subsequent solid samples

185   chemical determinations (see below). A further subsample of each sludge disk was

186   placed immediately into a centrifuge tube containing 5% zinc acetate solution for

187   sulfide determination. In addition, in July, 2011, a sample of fish feces was taken

188   from several fish together with samples of the fish feed for analysis.

189

190   The core sampled on July 13th, 2011 for pH measurements was brought back

191   to the lab and sludge samples were siphoned off from the top of the core into a

192   beaker in which pH was measured at the ambient temperature (~26°C). In addition,

193   one sample from the overlying water was taken for pH measurement.

194   The two cores collected on August 4th, 2011 (Core A) and February 2nd, 2012

195   (Core B) were immediately frozen after sampling and transported to Leeds with dry

196   ice. In Leeds, the cores were extruded frozen, cut into the required depth intervals

197   for analysis, and trimmed. The ice formed from overlying water at the top of each

198   core was melted for analysis and sulfate recovery. Each sample was split into two

199   and each refrozen. One aliquot was weighed, dried at 110˚C and reweighed to

200   determine water content. The other aliquot was placed frozen into a sealed

201   extraction cell and flushed with N_2. Pore-water components were extracted by

202   diffusional exchange (Bottrell et al., 2000; Spence et al., 2005) for chemical analysis

203   and recovery of sulfate as $BaSO_4$. Freezing of core may cause redistribution of

204   solutes during freezing; however the effects are minimized since the cores are sub-

205   sampled at a coarse resolution and completely thawed to extract solutes. Freezing

206   prevents both post-sampling oxidation of S species and physical disturbance/mixing

207   of the core during transport, each of which would introduce far greater artefacts.

208

209

210   ***2.3. Pore water and solid sludge determinations***

211

212   Pore water samples were determined for major cations and anions by ICP-AES and

213   ion chromatography. Samples used for analysis of cations were acidified with two

214   drops of HCl (37%). Deionized water was added to some of the samples to facilitate

215   the dissolution of any observed precipitate. Elemental concentrations were

216   measured using a Side-On-Plasma ICP-AES model 'ARCOS' (Spectro GmbH,

217   Germany). Samples for determination of nitrate, sulfate, chloride, and phosphate

218   were forced through Reverse Phase filters and through 0.25 µm membrane filters to

9

219   remove organic material. The above anions were determined using an ICS-3000 Ion

220   Chromatograph (Dionex Corporation, Sunnyvale, California), with an AS17 analytical

221   column, an AG17 guard column, and an ASRS-Ultra II Anion Micromembrane

222   Suppressor. Total ammonia (NH_3, NH_4^+), from here on referred to as ammonia, was

223   determined with the salicylate-hypochlorite method as described by Bower and

224   Holm-Hansen (1980). Dissolved sulfide was analysed on samples fixed with ZnAc

225   with the methylene blue method of Cline (1969).

226   Freeze dried sludge samples, feed and fish feces were analyzed for P

227   speciation using the procedure of Aspila et al. (1976) to determine total P and

228   inorganic P (and hence by difference: organic P). In addition, adsorbed P was

229   determined using the first step of the SEDEX P speciation procedure of Ruttenberg

230   (1992) involving extraction by $MgCl_2$. Extracted samples were determined for

231   phosphate using the molybdate blue reaction (Golterman et al., 1978). The standard

232   error (1s) of these analyses was adsorbed P 3% (n =12), inorganic P 8% (n=16) and

233   organic P 4% (n =16). An additional solid subsample of sludge was analyzed for

234   major elements on fused glass beads prepared from ignited powders using a sample

235   to flux ratio of 1:10 (Lithium tetraborate) on PANalytical XRF spectrometer at

236   University of Leicester, UK. Quantification of inorganic polyphosphate was

237   accomplished using a fluorometric technique based on the interaction of inorganic

238   polyphosphate with 4',6'-Diamidino-2-phenylindole (DAPI) (Aschar-Sobbi et al.,

239   2008; Diaz and Ingall, 2010). DAPI is commonly used as a stain for nucleic acid but

240   will also bind to polyphosphate, which is then detected using a combination of

241   incident and observed wavelengths optimized for polyphosphate (Aschar-Sobbi et

242   al., 2008). Inorganic polyphosphate of at least 15 P atoms in size is quantified

243   independently of chain length to a detection limit of 0.5 µM (Diaz and Ingall, 2010).

244   Typical errors associated with this technique are ± 15% (Diaz and Ingall, 2010).

245

246   For the isotope cores, after pore-water extraction, acid-volatile (AVS =

247   dissolved sulfides and solid monosulfides) and chromium reducible sulfur (CRS =

248   pyrite sulfur and elemental sulfur) were extracted from the solid phase and recovered

249   as a single CuS precipitate for isotopic analysis. The mass of S recovered was

250   determined titrimetrically (Newton et al., 1995). Residual sulfur in the solid phase is

251   presumed to be organic-bound S and was converted to $BaSO_4$ by Eschka fusion and

252   determined gravimetrically. In addition, the 'Red Sea salt' and Rehovot tap water

253   used to create half seawater conditions in the system were sampled. The Red Sea

254   salt was dissolved for chemical analysis and sulfate recovered as $BaSO_4$ for both S

255   and O isotopic analysis.

256   The oxygen isotopic composition of aqueous sulfate was determined on

257    $BaSO_4$ precipitates using the method described by McCarthy et al. (1998) and using

258   a VG SIRA 10 gas source isotope ration mass spectrometer. Data are reported as

259    $\delta^{18}O$ in per mille (‰) relative to the Vienna Standard Mean Ocean Water (V-SMOW);

260   reproducibility (2 x standard error), estimated from replicate analyses of standards, is

261   0.3‰ or better. Sulfur extracts and fish feed samples were quantitatively converted

262   to SO_2 by combustion at 1,150°C in the presence of pure oxygen (N5.0) injected into

263   a stream of helium (CP grade). The combustion gases were quantitatively converted

264   to N_2, CO_2 and SO_2 by passing them through tungstic oxide. Excess oxygen was

265   removed by reaction with hot copper wires at 850°C and water was removed in a

266   magnesium perchlorate or Sicapent trap. All solid reagents were sourced from

267   Elemental Microanalysis, UK, and all gases were sourced from BOC, UK. N_2

11

268   continued through the system unchecked, whilst CO_2 and SO_2 were removed from,

269   and re-injected into, the gas stream using temperature controlled

270   adsorption/desorption columns. The $\delta^{34}S$ was derived using the integrated mass 64

271   and 66 signals relative to those in a pulse of SO_2 reference gas (N3.0). These ratios

272   are calibrated to the international V-CDT scale using an internal laboratory barium

273   sulfate standard derived from seawater (SWS-3), which has been analysed against

274   the international standards NBS-127 (+20.3‰), NBS-123 (+17.01‰), IAEA S-1 (-

275   0.30‰) and IAEA S-3 (-32.06‰) and assigned a value of +20.3‰, and an inter-lab

276   chalcopyrite standard CP-1 assigned a value of -4.56‰. If samples were more ^{34}S

277   depleted than CP-1, the IAEA S-3 standard was used instead. The precision

278   obtained for repeat analyses of standard materials was generally better than 0.3‰

279    $\delta^{34}S_{REF}$ (1 standard deviation).

280

281   **3. Results**

282

283   ***3.1. Water analyses***

284

285   The water quality was determined weekly in the circulating water of the ZDS system

286   (Fig. S1). The detailed sampling took place on July 12th, when main water quality

287   parameters had stabilized and ammonia, phosphate, nitrate and nitrite values were

288   0.02 mM, 1.03 mM, 16.1 mM and 0.017 mM, respectively. The nitrate concentration

289   in the overlying water at the time of sampling (17.4 mM) was much higher than in the

290   surface sludge. There was a decrease in nitrate such that the nitrate concentration

291   below 20 cm was close to or below the practical limit of detection. The nitrate

292   decrease within the sludge can be explained by the fact that under anoxic conditions

12

293   nitrate is reduced by bacteria, which oxidise organic matter and other reduced

294   compounds.

295   Sulfate is also respired under anoxic conditions within the sludge. In order to

296   recognize biologically mediated changes in sulfate in the sludge, it was necessary to

297   compare its concentration to that of sodium since the former compound is found in

298   measurable amounts in the sea salt added to the system. There was a systematic

299   increase in Na observed with depth with values increasing from ~ 50% seawater

300   concentration at the surface to 4 times higher concentration at the base of the sludge

301   core (Fig. S2A). This increase was most probably caused by the specific manner in

302   which sea salt was added to the system prior to the experimental period. Salt was

303   added to the DB with a working volume of 2.9 m^3 (approximately 25% of the total

304   water volume in the system). Although intended to completely dissolve in the total

305   system water, it appears that as a result of this mode of salt addition, relatively more

306   salt accumulated in the bottom layers of the DB. Despite the high porosity of the

307   sludge (0.95 in the top layers and decreasing to 0.85 at 35 cm depth), there was no

308   evidence of physical mixing (Fig. S2C). Sulfate decreased rapidly from a value of

309   60.1 (SO_4 mM/Na M) in the overlying water to 14.8 (SO_4 mM/Na M) at 2.5 cm depth

310   (Fig. 2A). The ratio continued to decrease with depth to a minimum value of 4.3 (SO_4

311   mM/Na M) at 14.5 cm and then increased to 43.9 (SO_4 mM/Na M) at the lowest point

312   sampled (33.5cm). A similar profile was obtained when (total dissolved sulfur minus

313   dissolved sulfide)/Na was plotted with depth (Fig. 2A). There was no measurable

314   sulfide in the overlying water; it increased to a maximum of 3.8 mM at 15.5 cm and

315   then decreased to a value of 1.1 mM at 34.5 cm (Fig. 2B).

316   In order to understand the diagenetic processes in the sludge, the

317   concentration of relevant chemical species and parameters were measured.

13

318 Phosphate and ammonia are commonly measured as the products of the

319 heterotrophic anaerobic respiration of organic matter. However, the concentration of

320 these chemical species depends on the sum of all diagenetic processes in the

321 sludge. Thus, the dissolved phosphate in the sludge depth profile (Fig. 3A) was

322 lower in the uppermost layers (1.12 mM) compared with the overlying water (1.4

323 mM) and decreased with depth to values of ~0.7 mM at 35 cm. By contrast,

324 ammonia (Fig. 3B) was much higher in the surface sludge compared with the

325 overlying water. The ammonia concentrations in the upper 20 cm were roughly

326 constant in the range of 13-15 mM, which then decreased to ~10 mM below 25 cm.

327   Further information about the nature of the diagenetic processes in the

328 sediment comes from measurements of pH. In the sludge, the pH increased from

329 6.35 in the overlying water to a maximum of 6.8 just below the sediment water

330 interface (SWI) and then decreased with depth to a value of 6.5 at the base of the

331 sludge (Fig. S2D).

332   The concentration ratios of Ca/Na and Mg/Na were determined to provide

333 information about the possible precipitation of inorganic P minerals in the sludge.

334 The molar ratio in the overlying waters (21.96) was within error the same molar ratio

335 of Ca/Na (mM/M) in normal seawater (Fig. S2B). The ratio increased just below the

336 sludge-water interface to 40.7 and then decreased with depth reaching values of ~5

337 at 35 cm. The Mg/Na (mM/M) remained essentially constant at 60-78 over the depth

338 profile analysed (not shown).

339

340 ***3.2. Solid sludge phase***

341

342 The P speciation and content of the sludge was compared with feces (the major

343 input) and fish feed (a possible minor input) to characterise the transformations

344 which have occurred in the DB. The total P in the sludge varies from ~1,500

345 µmolesP/g in the surface layers increasing to a maximum of 2,090 µmolesP/g at 15.5

346 cm and decreasing to 1,100 µmolesP/g at the base of the sludge (Fig. 4A). Inorganic

347 P was the major phase in the sludge and increased from surface values of 1,030

348 µmolesP/g to >1,500 µmoles/g before decreasing to 1,120 µmoles/g at 35.5 cm. By

349 contrast, organic P was relatively constant over the upper 20 cm at ~400-500

350 µmolesP/g and then decreased to <50 µmoles/g at the base of the sludge (Fig.

351 4A).The total P content of the fish feed (410 µmolesP/g) was lower than the fish

352 feces (830 µmolesP/g), which is the main source of particulate matter to the sludge.

353 In contrast to the sludge, the organic P content of the fish feces (465 µmolesP/g)

354 was higher than its inorganic P content (260 µmolesP/g; Figure 4a; Table S1). The

355 principal major element in the sludge was Ca, which increased from 2.3 mmolesCa/g

356 (9.3 wt%Ca) at the surface to 3.2-4.1 mmolesCa/g (12.8-16.4 wt%Ca) at depth

357 (Table S2). Other elements, which might bind with P (Fe and Al), were present only

358 in µmoles/g concentrations (Table S2).

359

360 *3.2.1. Sulfur mass balance*

361 Sulfur mass balance can be assessed in the cores used for S isotopic

362 determinations as concentrations were also measured (Table 1). Data are presented

363 as aqueous concentrations for dissolved species and corrected to concentrations in

364 total sludge for all species (assuming a linear transition between measured

365 porosities of 0.95 at core top and 0.85 at core base). As noted above, sulfate

366 concentrations decline with depth in the upper part of the core (14.2 mM in the

15

367   overlying water, 7.8 mM in the uppermost core, declining to a minimum of 0.7 mM at

368   ~20 cm depth). However, although sulfide concentrations increase over a similar

369   interval (0 mM in the overlying water, 0.4 mM in the uppermost core, reaching a

370   maximum of 3.5 mM at ~17 cm depth) they never match the losses in sulfate and

371   thus total dissolved S decreases with depth over this interval. This imbalance is

372   explained by the general increase in concentration of solid phase S species over the

373   same depth interval (from ~590 mmol S/L of sludge in the upper core to >1,000

374   mmol S/L of sludge in the deepest core; Table 1), as sulfide reacts with solid phase

375   components to produce new organic S and CRS species. Elemental S may be a

376   product of sulfaide reoxidation (e.g. Jiang et al. 2009) and this is analyzed within the

377   CRS fraction.

378

379   **_3.3. Stable Isotope ratios_**

380   _3.3.1. Inputs to the system_

381   The 'Red Sea salt' used to make up the tank water contained sulfate with isotopic

382   compositions of $\delta^{34}S$ = -1.5‰ and $\delta^{18}O$ = 10.0‰ (Fig. 5); this is not a typical marine

383   sulfate isotope composition as the sulfate is sourced from terrestrial sulfate deposits.

384   The local Rehovot tap water used to fill the tank contains 0.16 mM sulfate with

385   isotopic composition of $\delta^{34}S$ = 6.9‰ and $\delta^{18}O$ = 7.8‰. As the circulating tank water

386   was made up to 50% seawater chloride concentration, the dissolved sulfate was

387   dominated by the added Red Sea salt. Fresh water resources (both groundwater and

388   river waters) in Israel typically have a narrow range of $\delta^{18}O$ between -4‰ and -6‰

389   (Gat and Dansgaard, 1972) and the tap water used should be in this range. The

390   other main source of S to the system was the fish food, which contains ~0.7 wt% S;

16

391   two different batches of food were analyzed and had slightly different δ^{34}S isotopic

392   compositions, 6.5‰ and 8.9‰ (Fig. 5).

393

394   *3.3.2. Solid phase sulfur isotopic composition*

395   The combined acid-volatile (AVS) and chromium reducible sulfur (CRS) content of

396   the sludge was similar in both cores and showed no systematic variation with depth,

397   ranging from 3.45 to 10.5 mg g^{-1}. Organic-S contents were lower (0.81 to 3.54 mg g^{-}

398   ^{1}) and again showed no strong depth trend (Table S3). Both forms of S in the sludge

399   show a similar and quite narrow range of S isotopic composition (AVS + CRS =

400   1.4‰ to 8.2‰; Org-S = 3.6‰ to 8.3‰, Fig. 5, Table S3) and no systematic variation

401   with depth. The S isotopic composition of pore-water sulfate was broadly similar in

402   both cores, particularly so in the upper part of each core (Fig. 5). The lowest δ^{34}S

403   value occurred in the shallowest pore-water sample and was lighter than the sulfate

404   in the overlying water (7.3‰ vs. 8.8‰ in core A and 8.0‰ vs. 10.2‰ in core B,

405   differences of 1.5‰ and 2.2‰). Below this, sulfate δ^{34}S remained near constant with

406   depth down to 17 cm and had values closely similar to the sulfate in the overlying

407   water. Below 17 cm depth the two profiles diverged somewhat, though in general

408   there was a tendency to higher δ^{34}S in the lower part of the profiles. Sulfate δ^{18}O in

409   the shallowest pore-waters was lower than in the overlying water but initially

410   increased with depth in both profiles. In the deeper pore-waters there is more

411   variability in sulfate δ^{18}O and Core A tended to more elevated values (>+10‰) while

412   core B tended to lighter values (~+2‰); it should be noted that SO_4/Cl was different

413   for the two cores in their deeper parts.

414

3.3.3. Calculation of the amount of total P in the sludge and the fraction accumulated during the present phase of pond operation

The total sludge volume was calculated to be 960,000 cm^3 based on a tank surface area of 2.4 m^2 and a depth of sludge of 40 cm. With an average sludge porosity of 0.9, it could be calculated that the DB contained 96,000 cm^3 of sediment particles. Assuming a dry density of 1.4 g/cm^3, this equals 134,400 g of sediment. Using 1,535 mmolesP/g as the average total P content of the sediment, it is calculated that the sludge contains 206 moles P. Our calculation of the total P supplied to the ZDS as fish feed minus the fish growth during the present run (October 2010 until July 2011) was 65 moles P. This figure assumes that the only location for P accumulation is the DB and that there was no major residual P build up in the nitrifying filter or elsewhere. As a result, this is a minimum estimate. Since P in the sludge cannot go anywhere, this implies that there were 141 moles of P already in the sludge before the system was started. The system had been operating for seven years intermittently before the start of this run. Therefore we conclude that the sludge before we started in October, 2010 was already a long term repository of P, built up during previous cycles of the ZDS system operating in a similar way to the present run.

3.3.4. Phosphate minerals within the sludge

The X-ray diffraction data of the freeze-dried but untreated core section and fish feces samples revealed a high background signal (due to high organic matter concentrations) with main peaks identifiable as calcite, fluorapatite and gypsum. The fish feed sample contained the same phases but with higher proportions of apatite and with additional calcium oxalates and hydroxyapatite (Fig. S3A). After the ashing

18

440   and washing all carbon phases (organic matter and calcite) as well as the highly

441   soluble gypsum were, as expected, absent from the scans (Fig. S3B). It is worth

442   noting that with XRD it was difficult to differentiate between the various, crystalline

443   forms of apatite (A) in these samples. However, a clear distinction between less

444   crystalline hydroxyapatite (HAP) and other Ca-P phases was observable but not

445   quantifiable due to the broadness of the peaks. Looking at the XRD scans of the

446   treated samples compared with the fish feces, which is the main source of organic

447   matter in the sludge, a clear difference can be seen in the nature of the Ca-P phases

448   present (Fig. S3B). There was a shift in the peak position for the apatite phases

449   (labeled A) to a lower angle and a decrease in peak height. The less crystalline HAP

450   peak also shifted to lower angles but increased in peak height and a new peak,

451   possibly assignable to Francolite (a carbonate rich form of fluor-apatite), appeared in

452   the sludge. Within the upper 13.5 cm of the sludge, the peaks for all Ca-P phases

453   remained relatively constant in both angle and relative magnitude. Between 19.5 cm

454   to 34.5 cm (data not shown) the peak locations remained constant though the

455   relative peak heights decreased somewhat. In none of the scans were there any

456   peaks that could be assigned to struvite.

457

458

459   **4. Discussion**

460

461   *4.1 P and N dynamics*

462

463   High concentrations of nitrate in the water flowing over the DB sludge on July

464   12th (17.4 mM) compared to much lower concentration of nitrate just below the SWI

19

465   (0.6 mM; Fig. 3C) are consistent with intense microbial denitrification in the DB . In

466   addition to rapid and extensive denitrification, heterotrophic sulfate reduction caused

467   ~75% of the sulfate present in the overlying water to be reduced within the upper 2.5

468   cm of the sludge. This sulfate reduction resulted in an accumulation of free sulfide in

469   the pore waters up to a maximum of 3.8 mM at ~15 cm. Despite the build up of free

470   sulfide in surface layers of the sludge, no free sulfide was measured in the fish tank

471   or circulating water. Previous studies have shown that this was due to autotrophic

472   denitrification (especially in the fluidized bed reactor) and other sulfide oxidation

473   processes efficiently removing any sulfide, which might leak from the sludge (Cytryn

474   et al. 2005; Neori et al., 2007; Sher et al., 2008; Schwermer et al., 2010; Neori and

475   Mendola, 2012).

476   In this study, we have used measurements of stable isotopes of S and O

477   ($\delta^{34}S$ and $\delta^{18}O$) in the solids and pore waters of the sludge tank to examine the

478   nature of the microbial processes in the DB. Water sampled from the system

479   (overlying water and pore water) contains sulfate that has significantly higher $\delta^{34}S$

480   than the sulfate initially added to the system (i.e. ~ 10‰ vs. -1.4‰). This results from

481   a combination of two effects: (1) during the operation of the system, fish feed with a

482   more elevated $\delta^{34}S$ has been constantly added and processing of this sulfur may

483   have added sulfate with higher $\delta^{34}S$ to the sulfate pool and (2) at the present time, S

484   accumulating in the solid phase (both as AVS+CRS and Org-S) has lower $\delta^{34}S$ than

485   the sulfate in the system (Fig. 5). If this solid phase pool has gradually accumulated

486   S with lower $\delta^{34}S$ than the contemporaneous sulfate, then this will have driven the

487   aqueous sulfate to progressively higher $\delta^{34}S$.

488   The $\delta^{34}S$ of pore-water sulfate in the upper 17 cm varies little from that of the

489   overlying water. However, the chemical data for pore-waters show large decreases

490 in SO_4/Cl in the upper parts of both cores, which would normally imply removal of

491 sulfate by microbial sulfate reduction. This process is usually accompanied by a

492 large sulfur isotope fractionation (e.g. Canfield 2001) with sulfide produced typically

493 20‰ to 45‰ depleted in ^{34}S compared to sulfate. However, in this particular reactor

494 this process seems to operate with much smaller fractionation. Firstly, there is only a

495 small offset between pore-water sulfate compositions and average solid phase

496 sulfide, with only~5‰ depletion in ^{34}S in the sulfide product and secondly there is no

497 large systematic increase in sulfate δ^{34}S as SO_4/Cl falls in the upper parts of both

498 cores (data not shown but similar to the SO_4/Na profile (Fig 2A). However, the

499 sulfate in the pore-water is not inert, as there are large changes in sulfate δ^{18}O over

500 this interval in both profiles (Fig. 5). Rather, sulfide produced must be near-

501 quantitatively reoxidized to sulfate and there is little net conversion of sulfate to

502 reduced forms such as AVS, CRS or Org-S (e.g. Bottrell et al., 2009). However, as

503 sulfate is reduced and reoxidized the re-formed sulfate contains oxygen atoms from

504 different sources and with different δ^{18}O to the original sulfate. The fact that sulfate in

505 the shallowest pore-water has slightly lower δ^{34}S than the overlying water or deeper

506 pore-water indicates that production of sulfate by reoxidation of ^{34}S-depleted sulfide

507 dominates at this level. The δ^{18}O of this sulfate is lower than the overlying waters (by

508 6.8‰ in Core A and 4.0‰ in Core B, Fig. 5). Such a shift to lower δ^{18}O in sulfate

509 rules out molecular oxygen as the oxidizing agent as it is highly ^{18}O enriched, but

510 rather indicates that the oxygen atoms incorporated into sulfate during sulfide

511 oxidation are derived from water molecules with negative δ^{18}O (McCarthy et al.,

512 1998; Bottrell and Tranter, 2002; Bottrell et al., 2009) and thus sulfide oxidation was

513 driven by an alternative electron acceptor, most likely nitrate, based on the chemical

514 profiles (Fig. 3C). Thus, it is concluded that in the upper layers of the DB there is

515   rapid heterotrophic sulfate reduction, which is approximately balanced by autotrophic

516   nitrate reduction. Heterotrophic nitrate reduction is a relatively lesser process. To test

517   the feasibility of such a scenario the system was investigated using a simple model

518   of the fate of S and N species.

519   The model considers the budgets of sulfur and nitrogen species in a system

520   where heterotrophic sulfate reduction (HSR), heterotrophic nitrate reduction (HNR)

521   and autotrophic nitrate reduction (ANR, using sulfide as an electron donor) may

522   occur. Starting compositions were those of the overlying water (15 mM sulfate, 15

523   mM nitrate and zero sulfide); reactions were modelled as first-order with respect to

524   these components. Concentration of organic substrate for heterotrophic respiration

525   was not considered to limit those reactions. The model describes the evolution of an

526   aliquot of pore-water as its composition is modified by these reactions. Model runs

527   were performed with different ratios of reaction rates, i.e. R_{HSR}/R_{HNR} and R_{ANR}/R_{HNR}.

528   Because sulfate is a lower energy-yielding electron acceptor, under similar

529   conditions R_{HSR} is generally lower than R_{HNR}, so all runs were made with R_{HSR}/R_{HNR}

530   ≤ 1. Experimental determination of the effect of sulfide on nitrate reducing systems

531   shows that $R_{ANR} > R_{HNR}$, with autotrophic activity often effectively eliminating

532   heterotrophic activity as long as sulfide is present (e.g. Sher et al., 2008; Shijie et al.,

533   2010), so all model runs were made with $R_{ANR}/R_{HNR} \geq 1$.

534   Model results are presented in Table 2. During most runs initially

535   heterotrophic NR dominated, but as sulfide concentration increased due to SR, rates

536   of autotrophic NR increased and became dominant (except in runs with very low

537   heterotrophic SR/heterotrophic NR where nitrate was consumed before autotrophic

538   NR became dominant). Where the rate of autotrophic NR is much greater than that

539   of heterotrophic NR, little nitrate is consumed by heterotrophic NR before autotrophic

22

540 NR becomes dominant and sulfide concentrations are low (and sulfate

541 concentrations remain high) until all nitrate is consumed. Thus, under many realistic

542 scenarios the system evolves such that SR is the dominant heterotrophic respiration

543 mechanism and the sulfide generated then accounts for the majority of NR via an

544 autotrophic pathway. This pattern is consistent with the observed chemistry and

545 stable isotope compositions that show that sulfate is cycled but not consumed in the

546 sludge over the interval where nitrate is consumed. Also shown in Table 2 are the

547 sulfide concentrations at which autotrophic NR becomes dominant; these are lower

548 than the observed concentrations in the sludge profile, indicating that ample sulfide

549 is available to drive autotrophic NR. Sulfide concentrations rise in the model runs

550 after nitrate concentrations fall, conditions similar to those observed deeper in the

551 sludge profile.

552

553 *4.2. Sediment sludge as a long term sink for P*

554

555 The digestion basin is a bacterial bioreactor in which the sediment sludge is

556 predominantly a repository of organic rich fish feces from the fish basin. Inputs to the

557 DB are modified subsequently mainly by anaerobic bacterial processes with the

558 major bacterial transformations described above. Despite the high fraction of organic

559 P in the fish feces input most of the particulate P in the DB is not organic P but

560 inorganic P (Fig. 4A, Table S1). X-Ray diffraction data indicates that the P

561 accumulating in the DB is a mixture of crystalline apatite and poorly ordered

562 hydroxyapatite (Fig. S3). There was no evidence of struvite. The XRD data,

563 however, showed that the fish feed contained large amounts of crystalline apatite

564 and some hydroxyapatite (probably as ground up fish bone from the fishmeal; Fig.

23

565 S3A) besides oxalates and calcite. Part of this initial apatite probably survives

566 through the gut of the *Sparus aurata* and is excreted within the fish feces (Fig. S3B,

567 top XRD scan). We ask the question whether the apatite measured in the sludge is

568 simply the residue of accumulating apatite supplied externally alone or whether it is

569 also formed actively in the sludge by *in situ* processes. The sludge in the uppermost

570 layer represents most closely the (transformed) fresh organic matter input from the

571 fish tank. We assume initially that the particulate matter reaching the sludge surface

572 was 100% fish feces because of good evidence for this based on observations and

573 on the observed fish growth, i.e. that the fish ate essentially all the food they were

574 fed. The total P measured in the surface sludge was 1,520 µmolesP/g, which is

575 higher in total concentration than either the fish feces (830 µmoles/g) or the fish feed

576 (410 µmoles/g; Table S1). It is known that there is significant denitrification and loss

577 of C by CO_2 and/or methane production in the ZDS system. Neori et al. (2007)

578 estimated that over a period of 500 days approximately 70% by weight was lost from

579 the system as gaseous nitrogen and carbon dioxide. The calculated loss of weight in

580 the conversion of 832 µmolesP/g to 1,520 µmolesP/g is 46% assuming that the total

581 P remained constant. This change in concentration for a period of 220 days was

582 reasonable based on the results of Neori et al. (2007) for a similar ZDS system. If we

583 assume that all of the change in measured inorganic P was only due to this loss of

584 total mass then the inorganic phase should be 480 µmolesP/g compared with the

585 measured inorganic P (1035 µmolesP/g) and the organic P was calculated to be 850

586 µmolesP/g compared with the measured 480 µmolesP/g of organic P. Thus, in

587 addition to any changes in concentration caused by loss of mass, there also had to

588 be a major and rapid conversion of organic P to inorganic P.

24

589 The sludge tank is a location of active heterotrophic nitrate and sulfate

590 reduction. There was major accumulation of ammonia and phosphate in the pore

591 waters (Fig. 3), an increase in pH (Fig. S2D) as well as rapid reduction in nitrate and

592 sulfate, which are all characteristic of heterotrophic bacterial reduction. However in

593 the upper 10 cm, which is the zone of most active heterotrophic reduction, while

594 ammonia increased with depth by ~ 2 mM, phosphate decreased by ~0.2 mM. This

595 requires a process within the upper layers of the sludge, which caused a net removal

596 of phosphate while ammonia (and presumably phosphate) was being released by

597 heterotrophic reduction. Phosphate could be removed by the formation of

598 polyphosphate granules in denitrifying and other reducing bacteria. However while

599 polyphosphate was present in the upper 10 cm, it was only found in µmoles/g

600 amounts (Fig. 4B) which was not sufficient to explain this major removal of

601 phosphate unless this represented a transient phase. A more likely explanation is the

602 formation of mineral apatite. Struvite, another possible mineral that could be

603 removed in such systems, would require the removal of both ammonia and

604 phosphate simultaneously. Our high-resolution X-Ray diffraction scans over the 50-

605 55° 2θ range (which is a location where apatite can clearly be separated from

606 hydroxyapatite and other Ca-P phases) showed the presence of hydroxyapatite

607 peaks in both the fish feces and the sludge. However, as described above, there was

608 a clear change in the nature and proportions of the crystalline and poorly ordered

609 Ca-P phases with depth (Fig. S3B) indicating that new, secondary Ca-P phases –

610 most likely additional hydroxyapatite and maybe francolite have formed. It needs to

611 be noted that the input of crystalline apatite from the fish feces and possibly also the

612 fish feed makes a quantitative determination of these changes difficult.

25

613   Using our measured pore water concentrations, the degree of saturation of

614   the pore waters for possible insoluble chemical species was carried out using

615   PHREEQC thermodynamic software in the upper layers of the sediment sludge. In

616   addition to measured pore water species (Fig. 3), we assumed a fluoride

617   concentration of half that in normal seawater (based on the Na and Cl concentrations

618   which are similar conservative elements and are measured as half seawater

619   concentration). The bicarbonate concentration was obtained from DIC

620   measurements on gel probes corrected for incomplete back equilibration assuming

621   that Cl and bicarbonate were equally affected. The calculation showed that the pore

622   waters were supersaturated with respect to hydroxyapatite, aragonite, calcite and

623   dolomite but not with respect to anhydrite, gypsum or struvite (Table 3).

624   Over the same depth interval (0-17 cm) as phosphate decreases by 0.2 mM

625   (Fig. 3), dissolved Ca decreases by 6 mM and the Ca/Na ratio decreased from 40 to

626   ~10 (Fig. S2B) while solid phase Ca increased from 2.33 mmolesCa/g to 4.24

627   mmolesCa/g (Table S2) and inorganic carbonate-C increased by a factor of 2 (Fig.

628   S2E). This means that ~15% of the Ca in the sludge is $CaCO_3$ (assuming that all

629   inorganic C is $CaCO_3$) and the remainder is apatite. Taken together, these data

630   suggest that these upper layers of the sludge are the site of active precipitation of

631   both hydroxyapatite and calcite from the pore waters of the sludge. The precipitation

632   of hydroxyapatite is facilitated in this system because not only were the pore waters

633   highly supersaturated with respect to apatite but also there were available apatite

634   nuclei in the shape of the ground up fish bones added via the fish food. Attempts to

635   observe directly the nature of the apatite formation process using XANES

636   measurements using synchrotron were not successful mainly because there were

simply too many phosphorus-rich granules in the observed field to observe the

necessary subtle changes in peak shapes predicted.

Our data also shows that in the longer term there was a conversion of organic

P to apatite within the digestion basin. At the time of the start up of this particular

ZDS run, there was sludge in the DB, which was the residue from seven years of

pond operation in various different modes i.e. different masses and sizes of fish but

fundamentally still being operated as a ZDS system. This residual sludge was

expected to contain the end products of ZDS processes. The observed depth profile

of the sludge showed an increase in inorganic P (i.e. apatite P) with depth and a

synchronous decrease in the proportion of organic P within the system particularly in

the lower layers (> 25 cm) where the almost all of the organic P appears to have

converted in a process analogous to the sink switching observed in recent marine

sediments (Ruttenberg and Berner, 1993) into inorganic apatite.

4.3. Synthesis comparing processes in DB to other systems

The ZDS was designed to use natural bacterial processes found in marine systems,

particularly in marine sediments, to control water quality conditions over long periods

of time (several months to years). These processes, which include nitrification, oxic

respiration, heterotrophic nitrate and sulfate reduction and autotrophic nitrate

reduction by sulphide, are balanced in such a way as to keep the water quality

conditions in the fishpond within levels acceptable for fish growth. Our results here

suggest that the closest natural analogue for P cycling processes in the DB are the

sediments beneath modern upwelling regions such as off Namibia and in the Arabian

Sea (e.g. Goldhammer et al., 2011; Schenau et al., 2000). These are sediments with

662   very high levels of organic matter (up to 40% OM). They are locations with intense

663   rates of heterotrophic bacterial respiration including both oxic processes and sulfate

664   reduction. The sediments underneath upwelling currents are the major areas for

665   phosphorite (apatite) formation. Schenau et al. (2000) observed high rates of

666   authigenic apatite formation, which they suggest, are induced by high rates of

667   organic matter degradation producing phosphate in the pore waters. They also

668   suggest that dissolution of fish debris acts as an additional source of dissolved

669   phosphate. The high concentration of dissolved phosphate together with normal

670   levels of calcium in the pore waters result in sufficient over saturation with respect to

671   apatite (francolite) precipitation to overcome the kinetic barrier known to exist in less

672   organic rich 'normal' marine sediments (van Cappellen and Berner, 1991).

673   An alternative mechanism for apatite precipitation has been suggested by

674   Goldhammer et al. (2010; 2011) who suggest that polyphosphate present in sulfide

675   oxidizing bacteria is rapidly converted to apatite. This process occurs under anoxic

676   conditions and they calculate that the rate of phosphate to apatite conversion by this

677   process exceeds the rate of phosphorus release during organic matter

678   mineralisation. It is possible that both of these processes are occurring in the DB

679   since there is direct evidence of both heterotrophic breakdown of organic matter and

680   extensive oxidation of sulfide and the presence of polyphosphate in the upper most

681   active layers of the DB. It is however not possible with the data collected in this study

682   to determine which of these processes dominate in the formation of apatite.

683   The phosphate that is removed from the recirculating system and

684   accumulates in the DB is mineral apatite. Apatite is the form of phosphate, which is

685   most commonly used as the primary mineral for commercial phosphate applications.

686   In a world with dwindling exploitable reserves of phosphorite and other phosphate

687   minerals it is important to recycle phosphorus. Since apatite is acid soluble, the

688   conversion of solid apatite from the sludge into dissolved P would be relatively easy.

689   Thus the P accumulated in this system could be easily recovered and converted into

690   a form of phosphorus that could be used in such applications as fertilizers.

691

702

703

704   **Appendix A. Supplementary data**

705

706   **REFERENCES**

707   Aschar-Sobbi, R., Abramov, A.Y., Diao, C., Kargacin, M.E., Kargacin, G.J.,

708   French,R.J., and Pavlov, E., 2008. High sensitivity, quantitative measurements

709   of polyphosphate using a new DAPI-based approach. Journal of Fluorescence

710   18, 859-866 DOI: 10.1007/s10895-008-0315-4.

711 Aspila K.I., Aqemian, H., Chau, A.S.Y., 1976. A semi-automated method for the

712   determination of inorganic, organic and total phosphate in sediments. Analyst

713   101, 187-197.

714 Barak, Y., van Rijn, J., 2000a. Biological phosphorus removal in a prototype

715   recirculating aquaculture system. Aquacultural Engineering 22, 121-136.

716 Barak, Y.,van Rijn, J., 2000b. Atypical polyphosphate accumulation by the denitrifying

717   bacterium *Paracoccus denitrificans*. Applied and Environmental Microbiology 66,

718   1209-1212.

719 Barak, Y., Cytryn, E., Gelfand, I., Krom, M., van Rijn, J., 2003. Phosphate removal in

720   a marine prototype recirculating aquaculture system. Aquaculture 220, 313-326.

721 Bottrell, S.H., Tranter, M., 2002. Sulphide oxidation under partially anoxic conditions

722   at the bed of the Haut Glacier d'Arolla, Switzerland. Hydrological Processes 16,

723   2363-2368.

724 Bottrell, S.H., Parkes, R.J., Cragg, B.A., Raiswell, R., 2000. Isotopic evidence for

725   deep anoxic pyrite oxidation and stimulation of bacterial sulphate reduction.

726   Journal of the Geological Society 157, 711-714.

727 Bottrell, S.H., Mortimer, R.J.G., Davies, I.M., Harvey, S.M., Krom, M.D., 2009.

728   Sulphur cycling in organic-rich marine sediments from a Scottish fjord.

729   Sedimentology 56, 1159-1173.

730 Canfield, D.E., 2001. Isotope fractionation by natural populations of sulfate-reducing

731   bacteria. Geochimica et Cosmochimica Acta 65, 1117-1124.

732   Cytryn, E., Barak, Y., Gelfand, I., van Rijn, J., Minz, D. 2003.Diversity of microbial

733   communities correlated to physiochemical parameters in a digestion basin of a

734   zero-discharge mariculture system. Environmental Microbiology 5, 55-63.

735   Cytryn, E. , van Rijn, J. , Schramm, A. , Gieseke, A., de Beer, D., Minz, D., 2005.

736   Identification of bacterial communities potentially responsible for oxic and anoxic

737   sulfide oxidation in biofilters of a recirculating mariculture system. Applied and

738   Environmental Microbiology 71, 6134-6141.

739   Diaz J. and Ingall E.D., 2010. Fluorometric quantification of natural inorganic

740   polyphosphate.   Environmental Science and Technology 44, 4665-4671. doi:

741   10.1021/es100191h.

742   Gat, J.R., Dansgaard, W., 1972. Stable isotope survey of the fresh water

743   occurrences in Israel and the northern Jordan rift valley. Journal of Hydrology 16,

744   177-212.

745   Gelfand, I., Barak Y., Even-Chen, Z., Cytryn, E., Krom, M., Neori, A.,van Rijn, J.,

746   2003. A novel zero-discharge intensive seawater recirculating system for culture

747   of marine fish. Journal of the World Aquaculture Society 34, 344-358.

748   Goldhammer, T. ,Bruchert, V., Ferdelman, T.G, Zabel., M., 2010. Microbial

749   sequestration of phosphorus in anoxic upwelling sediments Nature Geoscience

750   3 (8), 557-561.

751   Goldhammer, T., Brunner, B., Bernaconi, S.M., 2011. Phosphate oxygen isotopes:

752   Insights into sedimentary phosphorus cycling from the Benguela upwelling

753   system. Geochimica et Cosmochimica Acta 75 (13), 3741-3756.

754 Golterman, H.L., Clymo, R.S., Ohnstad, M.A.M., 1978. Methods for Physical and

755   Chemical Analyses of Freshwaters, 2nd ed. (International Biological Programme

756   Handbooks; no. 8). Blackwell Scientific Publ, Oxford, U.K., 210 pp.

757 Jiang, G., Sharma, K.R., Guissola, A., Keller, J., Yuan, Z. 2009. Sulfur

758   transformation in rising main sewers receiving nitrate dosage. Water Research

759   43, 4430-4440.

760 McCarthy, M.D.B., Newton, R.J., Bottrell, S.H.,1998. Oxygen isotopic compositions

761   of sulphate from coals: implications for primary sulphate sources and secondary

762   weathering processes. Fuel 77, 677-682.

763 Naylor, R.L., Goldberg, R.J., Mooney, H., Beveridge, M.C., Clay, J., Folk, C.,

764   Kautsky, N., Lubchenco, J., Primavera, J.,Williams, M., 1998. Nature's subsidies

765   to shrimp and salmon farming. Nature 282, 883-884.

766 Neori, A., Krom, M.D., van Rijn, J., 2007. Biochemical processes in intensive zero-

767   effluent marine fish culture with recirculating aerobic and anaerobic biofilters.

768   Journal of Experimental Marine Biology and Ecology 349, 235-247.

769 Neori, A., Mendola, D., 2012. An anaerobic slurry module for solids digestion and

770   denitrification in recirculating, minimal discharge marine fish culture systems.

771   Journal of the World Aquaculture Society 43, 859-868.

772 Newton, R.J., Bottrell, S.H., Dean, S.P., Hatfield, D., Raiswell, R., 1995. An

773   evaluation of the chromous chloride reduction method for isotopic analyses of

774   pyrite in rocks and sediment. Chemical Geology 125, 317-320.

775   Ruttenberg, K.C., 1992. Development of a sequential extraction method for different

776   forms of phosphorus in marine sediments. Limnology and Oceanography 37,

777   1460-1482.

778   Ruttenberg K.C., Berner, R.A., 1993. Authigenic apatite formation and burial in

779   sediments from non-upwelling, continental margin environments. Geochimica et

780   Cosmochimica Acta 57, 991-1007.

781   Schenau, S., Slomp, C.P., DeLange, G.J., 2000. Phosphogenesis and active

782   phosphorite formation in sediments from the Arabian Sea oxygen minimum

783   zone. Marine Geology 169 (1-2), 1-20.

784   Schneider, K, Sher, Y., Erez, J., van Rijn, J., 2011. Carbon cycling in a zero-

785   discharge mariculture system. Water Research 45(7), 2375-2382.

786   Shijie, A., Tang, K., Nemati, M., 2010. Simultaneous biodesulphurization and

787   denitrification using an oil reservoir microbial culture: effects of sulphide loading

788   rate and sulphide to nitrate loading ratio. Water Research 44, 1531-1541.

789   Sher, Y., Schneider, K., Schwermer, C.U., van Rijn, J., 2008. Sulfide induced nitrate

790   reduction in the sludge of an anaerobic treatment stage of a zero-discharge

791   recirculating mariculture system. Water Research 42, 4386-4392

792   Schulz H.N., Brinkhoff T, Ferdelman TG, Marine M.H., Teske A., Jorgensen B.B.,

793   1999. Dense populations of a giant sulfur bacterium in Namibian shelf sediments.

794   Science 284, 493–495.

795   Spence, M.J., Thornton, S.F., Bottrell, S.H., Spence, K.H., 2005. Determination of

796   interstitial water chemistry and porosity in consolidated aquifer materials by

33

797   diffusion equilibrium-exchange. Environmental Science and Technology 39,

798   1158-1166.

799 Schwermer, C.U., Ferdelman, T.G., Stief, P., Gieseke, A., Rezakhani, N., van Rijn,

800   J., de Beer, D., Schramm, A., 2010. Effect of nitrate on sulfur transformations in

801   sulfidogenic sludge of a marine aquaculture biofilter. FEMS Microbiology and

802   Ecology 72, 476-484.

803 Van Cappellen, P., Berner, R.A., 1991. Fluorapatite crystal growth from modified

804   seawater solutions. Geochimica et Cosmochimica Acta 55, 1219-1234.

805 van Loosdrecht, M.C.M., Brandse, F.A.M., de Vries, A.C., 1998. Upgrading of

806   wastewater treatment processes for integrated nutrient removal – the BCFS

807   process. Water Science and Technology 37, 209-217

808 van Loosdrecht, M.C.M., Hooijmans, C.M., Brdjanovitch, D., Heijnen, J.J., 1997.

809   Biological phosphate removal processes. Applied Microbiology and

810   Biotechnology 48, 289-96.

811 van Rijn, J. 2013. Waste treatment in recirculating aquaculture systems.

812   Aquacultural Engineering 53, 49-56.

813

814

815

816 **Figure legends**

34

817   Figure 1. A diagram of the system as a whole including a more detailed diagram of

818   the digestion basin showing the location of the sludge sampling.

819   Figure 2. Pore water concentration of a) Sulfate/Na and {Total dissolved S

820   (measured by ICP) minus dissolved Sulfide} /Na concentration ratio

821   (mmolesS/moleNa) and b) Dissolved Sulfide (molesS/l) in the pore waters of the

822   sludge. Measured value for sulfate/Na molar ratio in the overlying water (OW) is

823   given. There was no sulfide detected in the overlying water.

824   Figure 3. Pore water nutrient concentrations of dissolved phosphate, ammonia and

825   nitrate vs depth together with corresponding values for these nutrients in the

826   overlying water. Note that the concentration of nitrate in the overlying water is 17.4

827   mM as noted in the data point description.

828   Figure 4.   Phosphate in sludge: (A) Changes in P speciation with depth in sludge of

829   the sedimentation basin together with the P speciation of the fish feces which is the

830   main input of particulate matter to the digestion basin; (B) Polyphosphate

831   concentrations (μmole/g) with depth.

832   Figure 5. Depth profiles of $\delta^{34}S$ and $\delta^{18}O$ of dissolved sulfate for two sludge cores

833   with depth. Also shown are $\delta^{34}S$ and $\delta^{18}O$ of sulfate in the overlying waters and

834   values for input sources (Red Sea Salt (RSS) and tapwater). On the left hand

835   diagram the ranges depicted in boxes are for solid phase S species in the core; CRS

836   = cromium reducible sulfur (monosulfides + pyrite + elemental S), Org S = organic

837   sulfur; $\delta^{34}S$ values are also plotted for fish feed.

838

839

840   Figure 1:

Trickling filter · Foam fractionator · Fish Basin · Swirl separator · Fluidized bed reactor · Foam · Sludge · Digestion basin · Intermediate collection basin · Sludge Sampling location · Out · In · Water layer · Sludge layer

pump
Aerobic water flow
Anoxic water flow
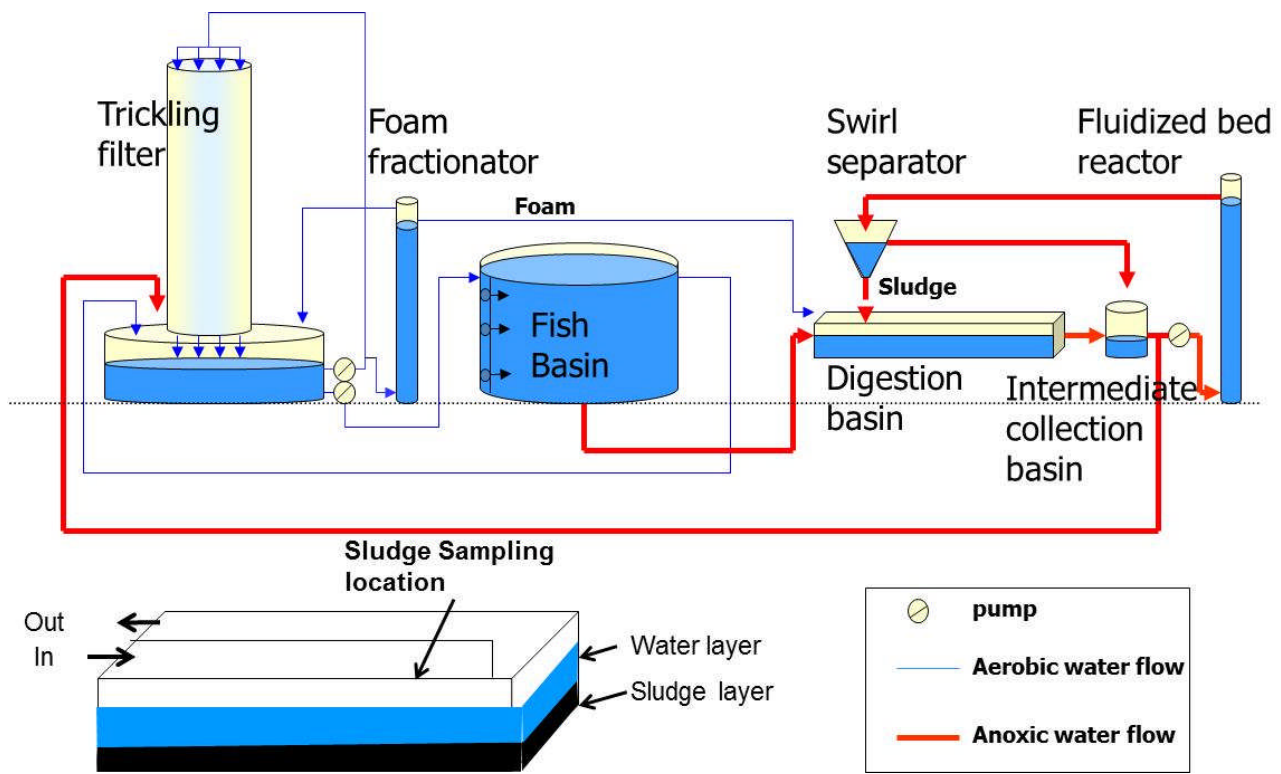
841
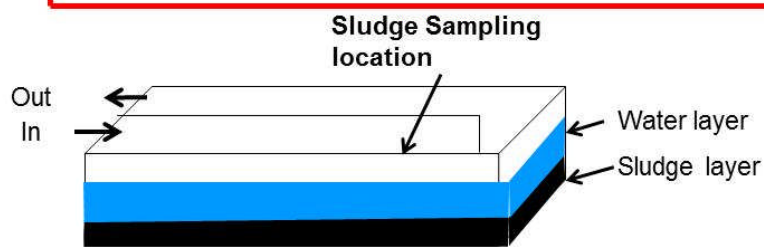
842

843

844

845

846

847

848

849

850

36

851   Figure 2:

852

853

854

855

856

37

857 Figure 3

858

859

Figure 4

861

39
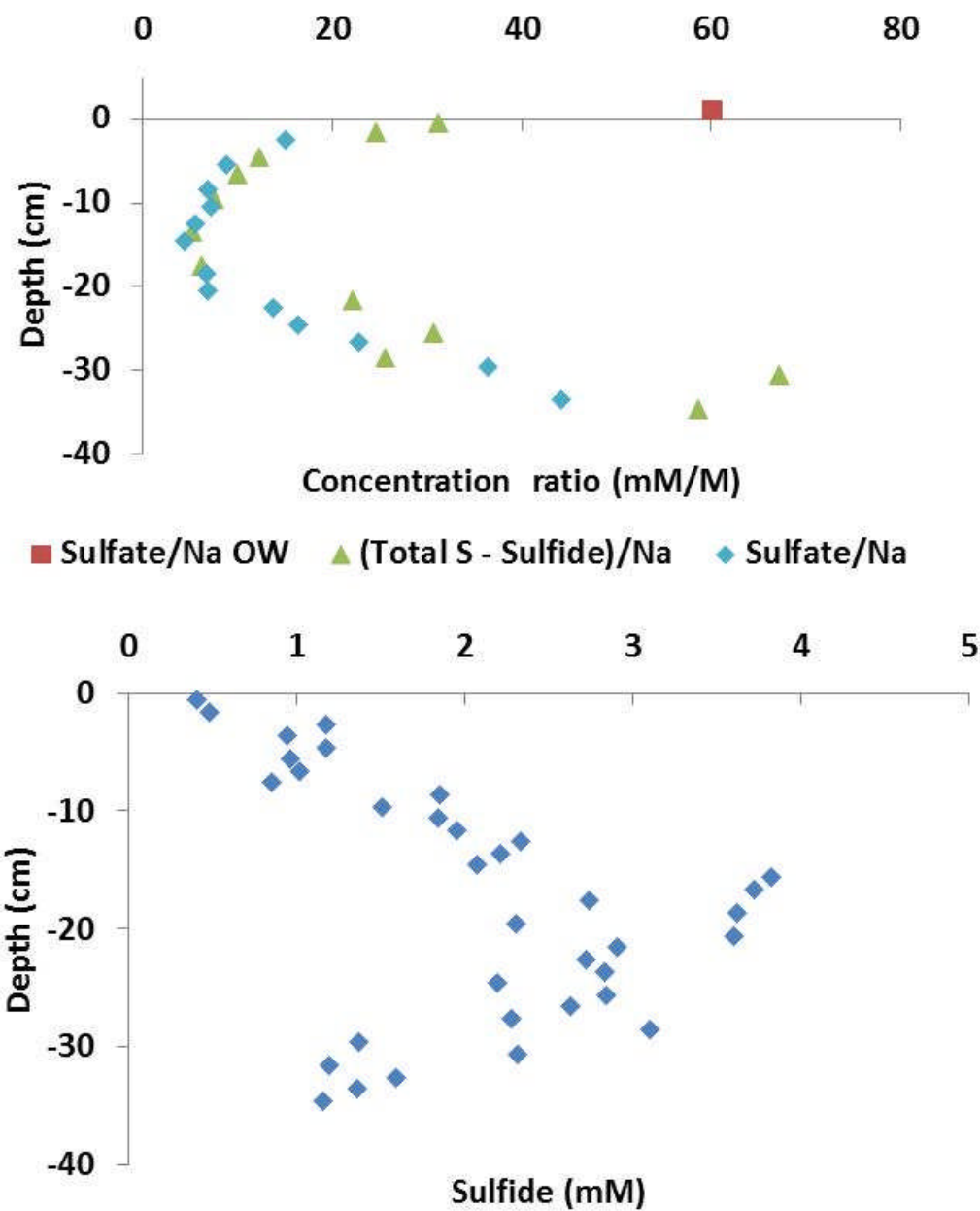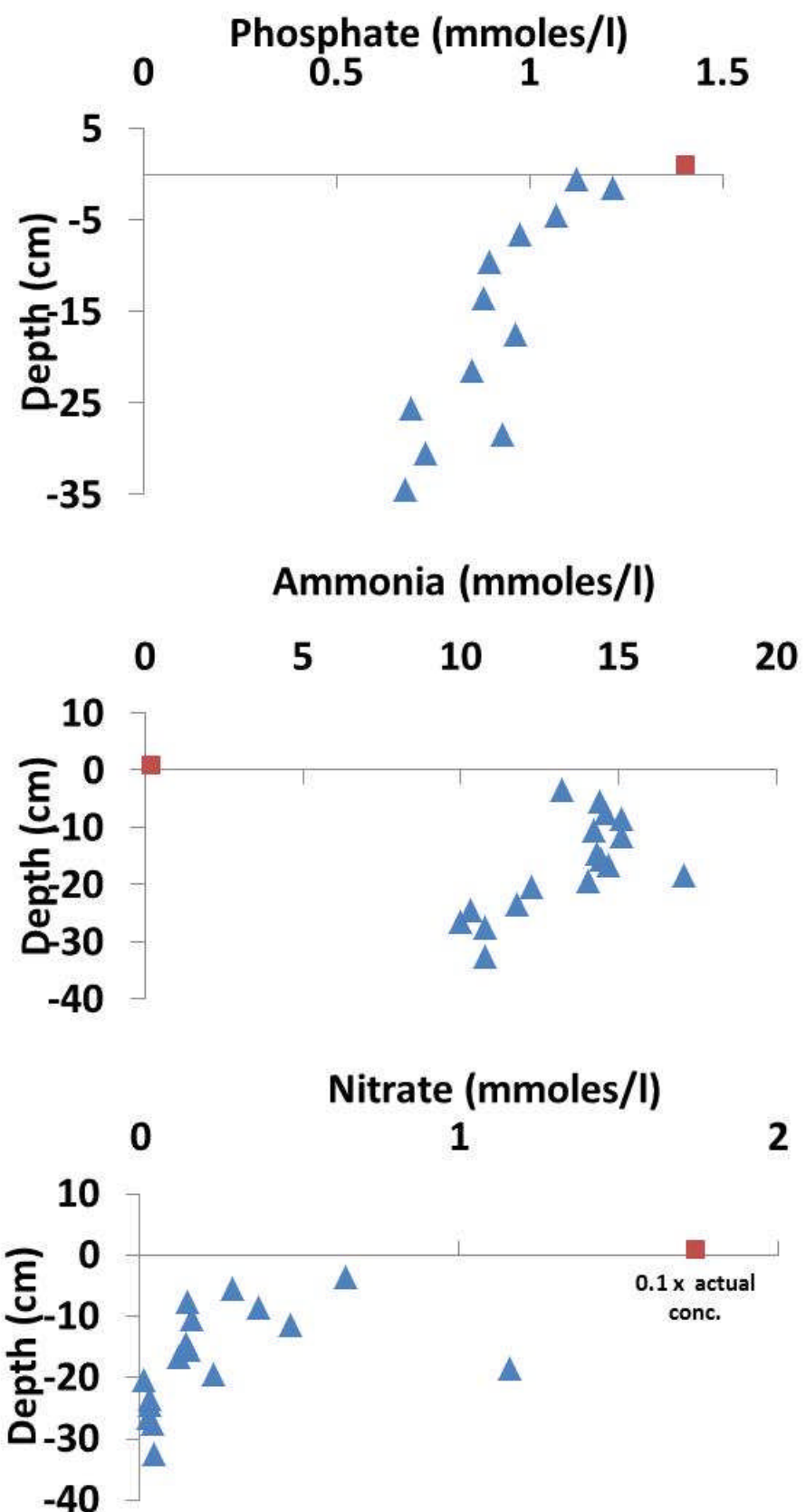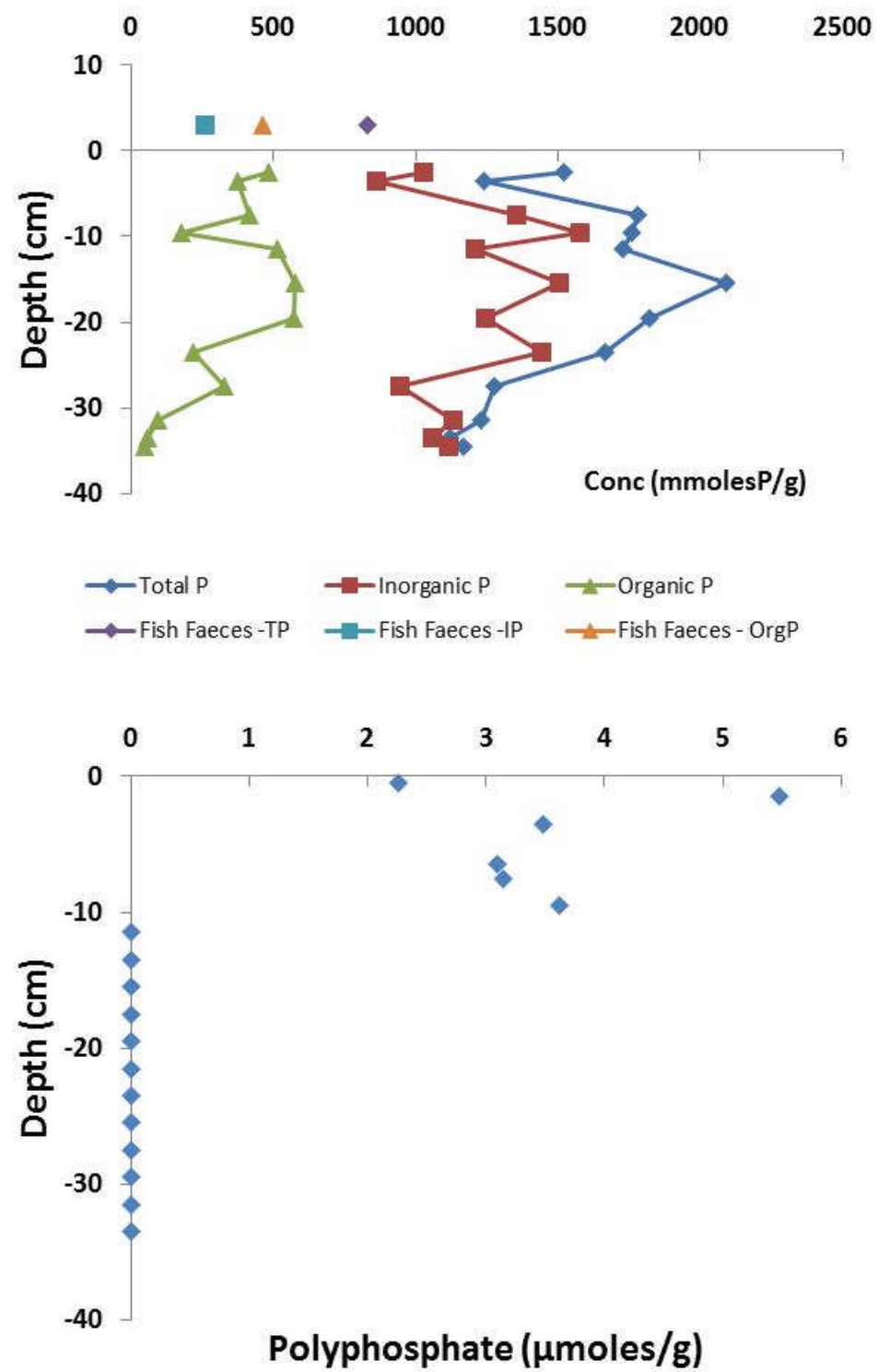
862

863
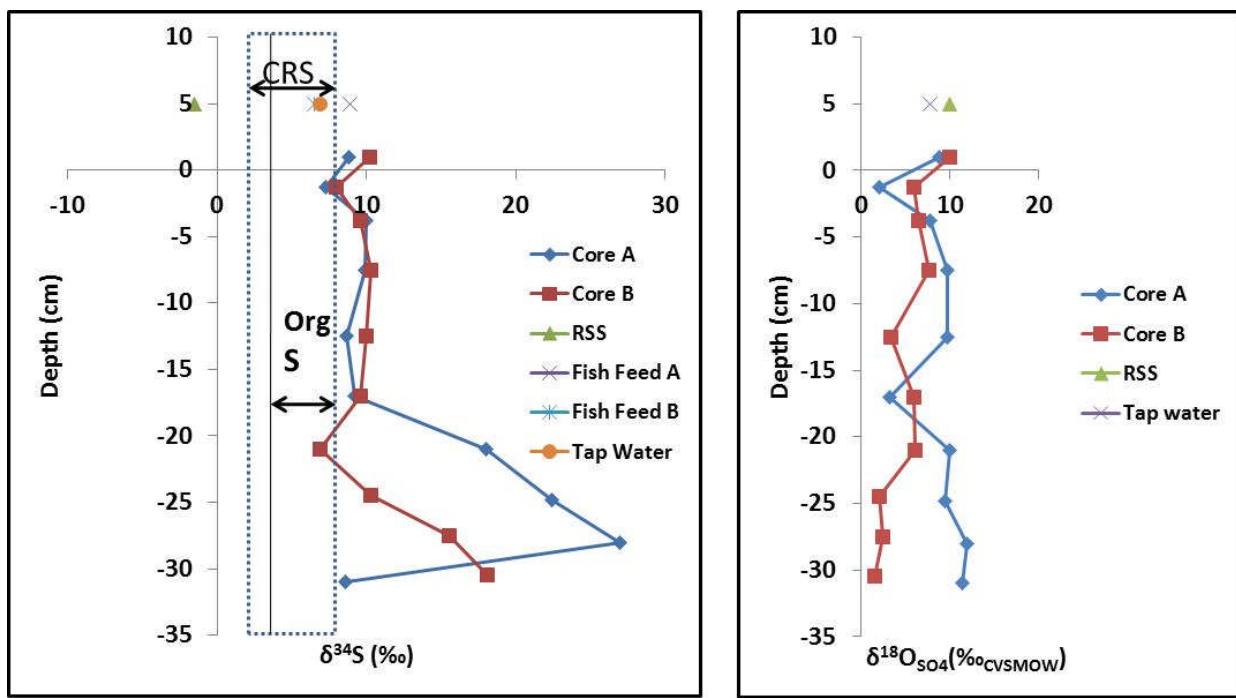
864

865   Figure 5

866

867

868

869

870

871

872

873

40

874

Figure S1

875

876

877

878

41
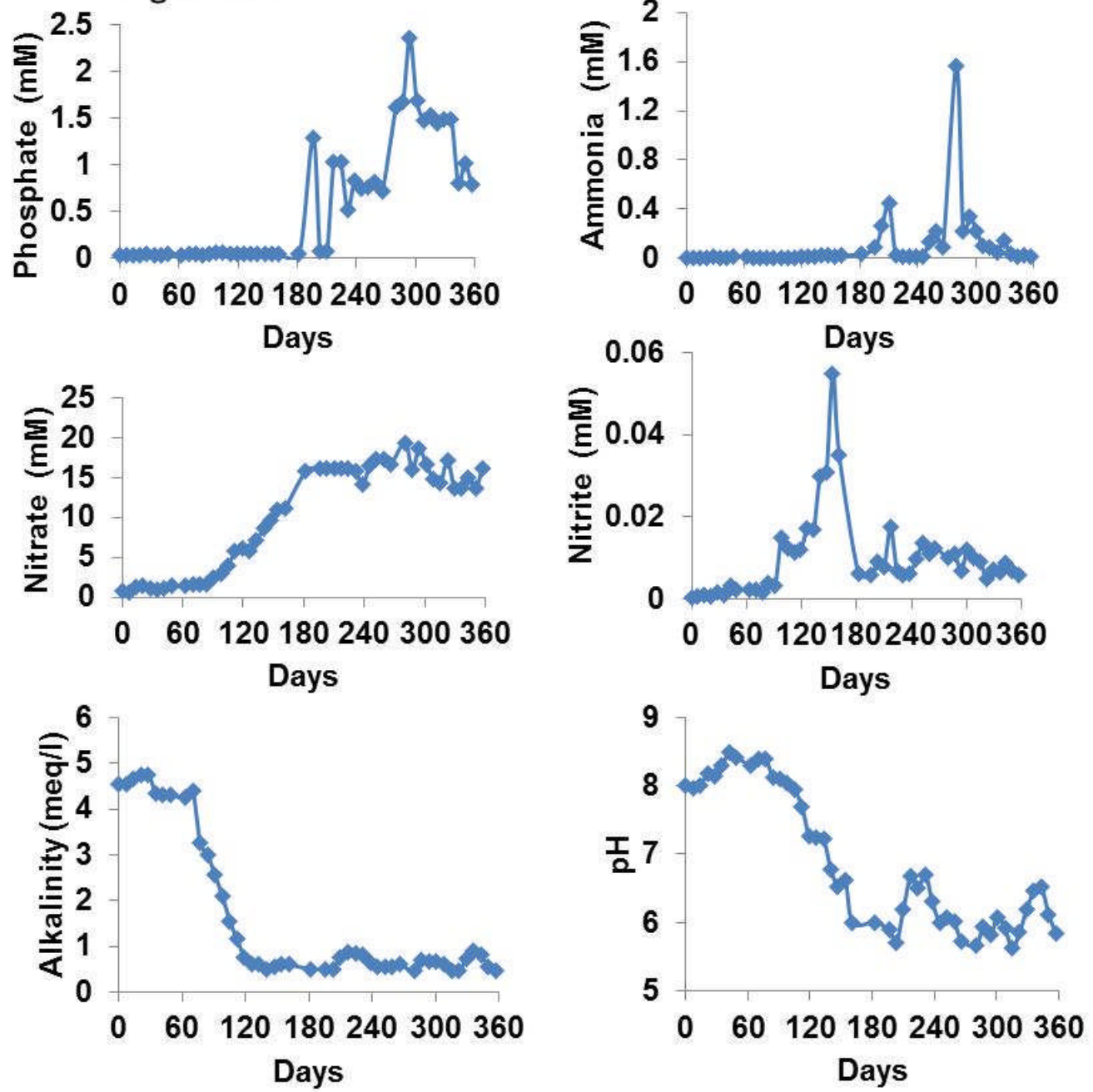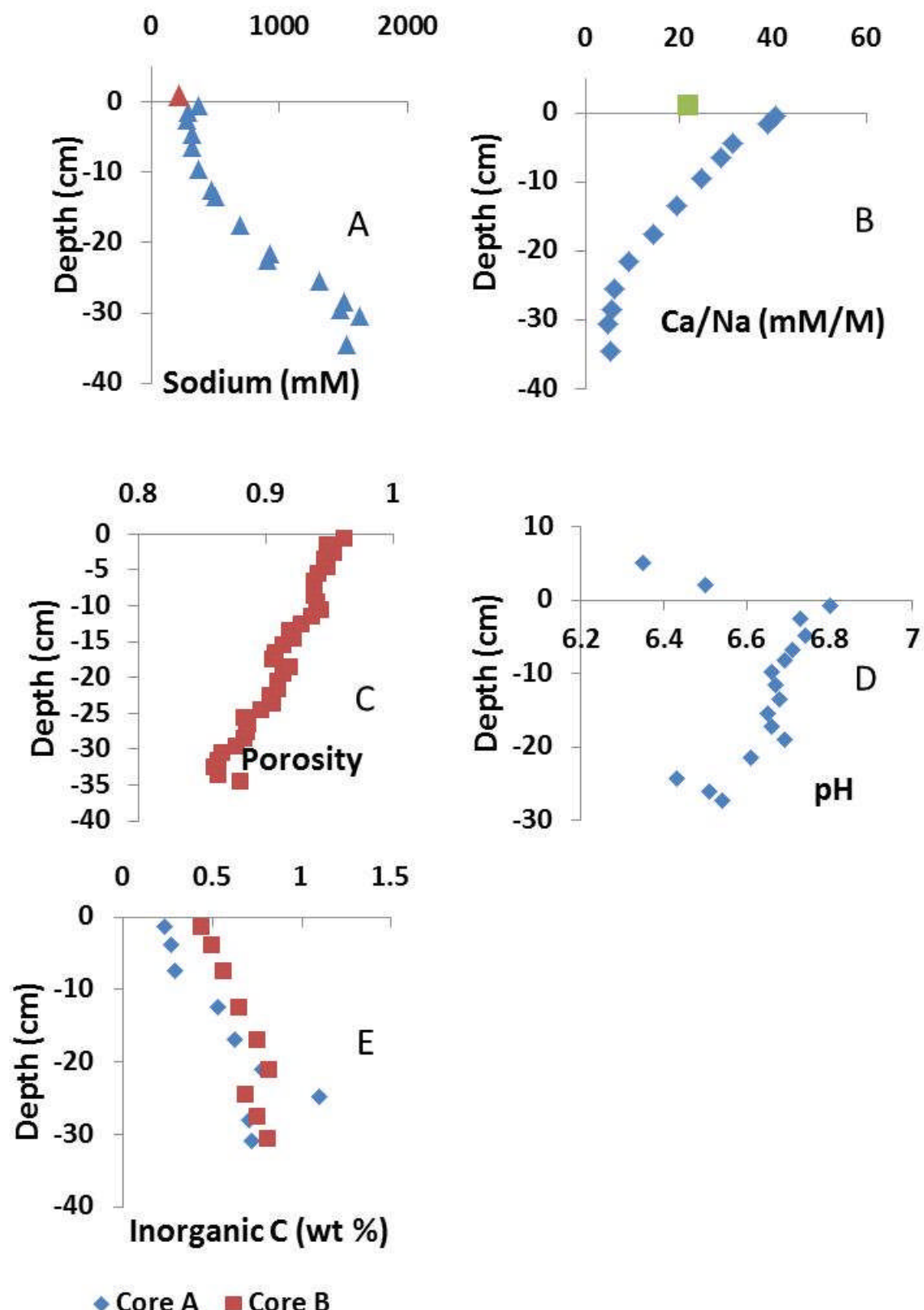
Figure S2

881

Figure S3A
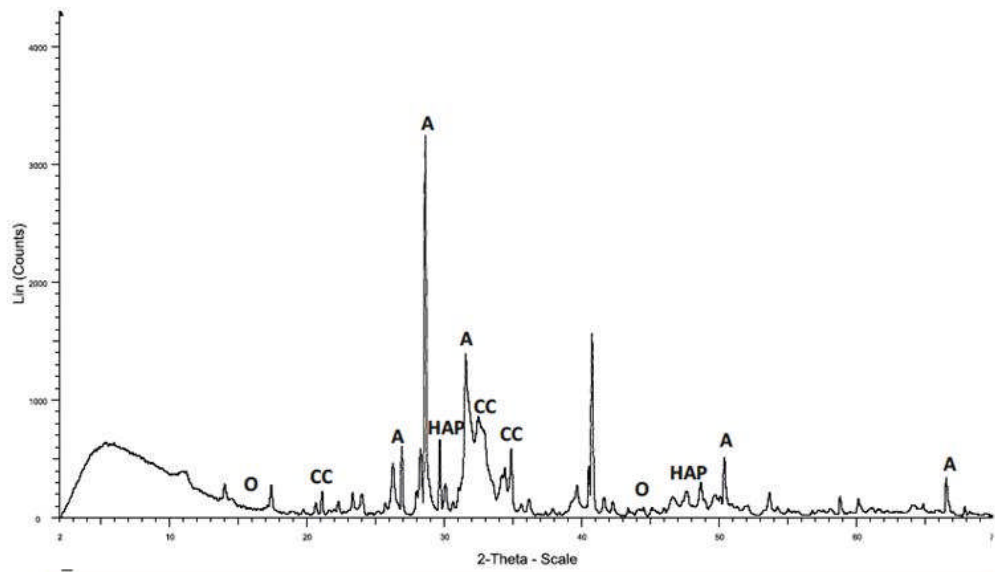
882

883

884

885

886

887

888

889

890

891

892

893

894

Figure S3B

Fish Faeces

F.?   HAP

Sample 72 (1.5cm)

Sample 68 (5.5cm)

Sample 64 (9.5cm)

Sample 60 (13.5cm)

895